

# Oscillations above sunspots from the temperature minimum to the corona

N.I. Kobanov, A.A. Chelpanov, and D.Y. Kolobov

Institute of Solar-Terrestrial Physics

of Siberian Branch of Russian Academy of Sciences, Irkutsk, Russia

email: kobanov@iszf.irk.ru

[This article was accepted for publication in *Astronomy&Astrophysics*]

## Abstract

**Context.** An analysis of the oscillations above sunspots was carried out using simultaneous ground-based and Solar Dynamics Observatory (SDO) observations (Si I 10827 Å, He I 10830 Å, Fe I 6173 Å, 1700 Å, He II 304 Å, Fe IX 171 Å).

**Aims.** Investigation of the spatial distribution of oscillation power in the frequency range 1–8 mHz for the different height levels of the solar atmosphere. Measuring the time lags between the oscillations at the different layers.

**Methods.** We used frequency filtration of the intensity and Doppler velocity variations with Morlet wavelet to trace the wave propagation from the photosphere to the chromosphere and the corona.

**Results.** The 15 min oscillations are concentrated near the outer penumbra in the upper photosphere (1700 Å), forming a ring, that expands in the transition zone. These oscillations propagate upward and reach the corona level, where their spatial distribution resembles a fan structure. The spatial distribution of the 5 min oscillation power looks like a circle-shape structure matching the sunspot umbra border at the photospheric level. The circle expands at the higher levels (He II 304 Å and Fe IX 171 Å). This indicates that the low-frequency oscillations propagate along the inclined magnetic tubes in the spot. We found that the inclination of the tubes reaches 50–60 degrees in the upper chromosphere and the transition zone.

The main oscillation power in the 5–8 mHz range concentrates within the umbra boundaries at all the levels. The highest frequency oscillations (8 mHz) are located in the peculiar points inside the umbra. These points probably coincide with umbral dots.

We deduced the propagation velocities to be  $28 \pm 15 \text{ km s}^{-1}$ ,  $26 \pm 15 \text{ km s}^{-1}$ , and  $55 \pm 10 \text{ km s}^{-1}$  for the Si I 10827 Å–He I 10830 Å, 1700 Å–He II 304 Å, and He II 304 Å–Fe IX 171 Å height levels, respectively.

# 1 Introduction

Sunspot oscillations in the lower solar atmosphere have been observed and discussed for many decades (Beckers and Tallant, 1969; Zirin and Stein, 1972; Giovanelli, 1972; Balthasar and Wiehr, 1990; Zhugzhda, Locans, and Staude, 1985; Lites, 1992; Tsiropoula, Alissandrakis, and Mein, 2000). The problem has turned out to be complicated (Bogdan and Judge, 2006; Thomas and Weiss, 2008). Despite some success in this field, we are still far from a comprehensive understanding of the wave processes in and above sunspots.

Chromospheric waves in sunspots are readily detected in the  $H\alpha$  and  $He I$  10830 Å lines. It was found that different oscillatory modes coexist and the dominant frequency changes from 6–7 mHz in the umbra to 1.5–2 mHz in the outer penumbra. One hypothesis to explain the observed wave behavior is the common source located in subphotospheric layers. The scenario is that the waves originate in the deep layers of the solar atmosphere and propagate upward along the magnetic field lines (Roupe van der Voort *et al.*, 2003; Kobanov, Kolobov, and Makarchik, 2006; Kobanov *et al.*, 2011; Bloomfield, Lagg, and Solanki, 2007). In this case, one expects a positive time delay for the waves observed at the upper and lower levels. Detecting such a delay is a complex task, and the results from different authors are not always consistent with one another (Kobanov *et al.*, 2011; Centeno, Collados, and Trujillo Bueno, 2009).

Recent progress in solar physics instrumentation has revived the interest in investigating sunspot oscillations. Multiwavelength studies of the 3 and 5 min waves are of main concern. Whereas at the photosphere-chromosphere level these waves are detectable in intensity and Doppler velocity signals, in the transition zone and the corona they are recorded in UV intensity.

Aschwanden *et al.* (1999) and Nakariakov *et al.* (1999) researched transverse spatial oscillations of coronal loops, whose footpoints were anchored in the photosphere. The oscillations studied in 171 Å (TRACE) were triggered by a flare and their mean period was found to be 280 s. De Moortel *et al.* (2002) suggested a relation between the 3 min oscillations observed in coronal loops above sunspots and the 5 min oscillations in neighboring loops. These authors interpret the 3 min oscillations as slow magnetoacoustic waves with a propagation velocity of 70–235 km s<sup>-1</sup>. Brynildsen *et al.* (2003) also identified them as upwardly traveling acoustic waves.

O’Shea, Muglach, and Fleck (2002) measured time delays for the 3 min waves detected at different heights and estimated the propagating speeds for TRACE 1700 and O III 599.6 Å to be in the range of 27–86 km s<sup>-1</sup>. They detected both upward

and downward propagating waves. The result appreciably depends on the slit position (pixel number). This significantly complicates interpretation of the time delays detected for the waves at different levels. Marsh and Walsh (2006) showed that the 3 min oscillations in the transition zone above sunspots are directly connected to the waves in coronal loops. They supposed that global  $p$ -mode oscillations are involved in the process.

There are controversial opinions on plume- and fan-structure connection with the 3 min umbral oscillations. Brynildsen *et al.* (2004) showed that the 3 min umbral oscillations are limited to small coronal regions coinciding with bases of umbral coronal loops. They argue that these oscillations are not connected to plumes, whereas Jess *et al.* (2012) found a direct connection of the 3 min oscillations to coronal fans. They showed that the sources of the 3 min oscillations in coronal fans are seen to anchor into photospheric umbral dots with enhanced oscillation power. Analyzing the 3 min oscillations, Reznikova and Shibasaki (2012) obtained contradictory results for two different sunspots. Wang *et al.* (2009) detected 12 and 25 min oscillations of intensity and line-of-sight (LOS) velocity in fan-like coronal structures above active regions in Hinode Extreme-Ultraviolet Imaging Spectrometer (EIS) data. They identified them as propagating slow magnetoacoustic waves.

The 3 min oscillations detected in the microwave range were found to replicate those recorded in the chromosphere of sunspots with a 50-second delay (Abramov-Maximov *et al.*, 2011). This implies that the waves propagate from the chromosphere of an umbra to the upper levels.

Attempts to find a direct connection between photospheric–chromospheric waves and coronal waves above sunspots have encountered difficulties. As a rule, instruments that obtain UV data to detect coronal waves do not observe in the  $H\alpha$  and  $He\text{ I } 10830\text{ \AA}$  lines that are well suited for such a task. To perform a joint analysis, one has to use data from ground-based telescopes. The connection between waves in the corona and the deeper levels can be searched by direct comparison of the signal variations and by studying their spatial and temporal properties both visually and using cross-correlation.

This paper presents an attempt to make a joint analysis of the oscillations in a sunspot detected by ground-based observations and the Solar Dynamics Observatory (SDO) simultaneously. The data cover several levels of the solar atmosphere from the temperature minimum to the corona. Spatial power distribution of different oscillations is of interest, as well as their time lags. We tried to identify the frequencies for which the power spatial distribution better reproduces fan structures in the  $171\text{ \AA}$  line.

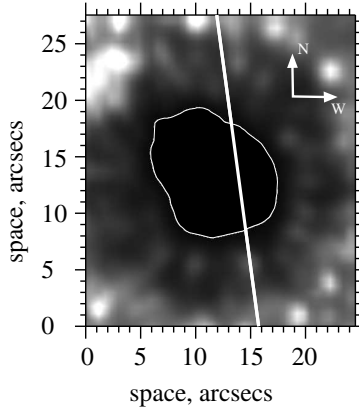


Figure 1: Spot NOAA 11479 in the  $1700 \text{ \AA}$  continuum. The position of the slit relative to the spot is shown with the straight white line. The closed curve denotes the umbra boundary in the white light.

The measurements of the time lag between the low-frequency oscillations at the different heights were performed taking into account the oscillation propagation trajectory inclination. We hope that this allows us to make more accurate wave propagation speed calculations.

## 2 Method and instruments

Two types of data were used in the research. First, we observed the sunspot NOAA 11479 (Figure 1) close to the disk center on 16 May 2012 for eight hours with a ground-based solar telescope at the Sayan Solar Observatory in two lines simultaneously:  $\text{Si I } 10827 \text{ \AA}$  and  $\text{He I } 10830 \text{ \AA}$ . They represent the upper photosphere and the chromosphere, respectively. The coordinates of the spot were N15E15 at the beginning of the observation, which corresponds to the small angle between the line of sight and the normal to the Sun's surface. The analysis was performed at different frequency bands, 1–3.5 mHz and 5–8 mHz.

The telescope resolution is usually about  $1''$  owing to the Earth's atmosphere. The telescope photoelectric guide tracks the solar image with  $1''$  accuracy for several hours of observations and compensates for image moving caused by the Sun's rotation.

One camera sensor element corresponded to the  $0.3''$  spatial resolution along the slit and  $30 \text{ m\AA}$  one along the spectrograph dispersion. The ultimate cadence

was one second after the summation of every ten frames.

We used the Doppler-compensator method to calculate the line-of-sight velocity for the Si I–He I pair. The wavelength position shift corresponds to the measured line-of-sight velocity variation (Kobanov *et al.*, 2009).

Also, we used for our analysis a series of Atmospheric Imaging Assembly (AIA) SDO data corresponding to the ground-based telescope observations. These observations comprise 6173 Å, 1700 Å, 304 Å, and 171 Å spectral bands, which represent the lower photosphere, the upper photosphere, the transition region, and the corona, respectively (Reznikova *et al.*, 2012).

To trace wave propagation from the photosphere to the chromosphere and the corona, we compared oscillations of the velocity and intensity signals filtered with Morlet wavelet. The time lags between the signals were determined by using the cross-correlation method.

We based our analysis on the following premises: a) in sunspots the upwardly propagating waves travel along magnetic field lines; b) registered periodic variations of line intensities in the lower atmosphere are caused by temperature variations; c) we use the line formation heights accepted in the current literature for the spectral lines that we chose.

### 3 Results

Spatial localization of different frequency oscillations is in close relation to the magnetic field topology in sunspots. Both the early works (Sigwarth and Mattig, 1997; Kobanov and Makarchik, 2004; Tziotziou *et al.*, 2006) and recent publications based on SDO data analysis (Reznikova and Shibasaki, 2012) note that low-frequency oscillations concentrate in regions where the magnetic field lines are significantly inclined (i.e., in the penumbra), whereas the 5 mHz and higher frequency oscillations are concentrated within the umbra boundaries.

First of all, we computed spatial distribution of the Fourier oscillation power for the 0.8 mHz spectral bandpass centered at 3.3 mHz (Figure 2). Only the pixels with oscillation power exceeding  $3\sigma^2$  level are plotted on the power spectrum maps (c-e). The darker a point, the higher is the oscillation power in it within the specified band pass. The closed curves denote the umbra border.

One can clearly see that the oscillation power is predominantly located in circle-shape structures; the areas of the circles increase with the line formation height. Proceeding from the assumption that these oscillations are manifestations of the magnetohydrodynamic waves propagating along the magnetic field

lines, we attempted to measure the inclination of the lines by visually matching the oscillation power maps in different bands. To determine more accurate spatial correspondence, we analyzed sequences of the filtered signal wave trains in the vicinities of the supposed correspondence points and found correlation coefficients for them (Figure 3a). Unambiguous correspondence was not found in every section along the umbra border, but in some points the cross-correlation coefficients reach 0.75. The mean displacement  $\Delta L$  of the circle structure boundaries is 2150 km (from 1800 to 3200 for different segments along the umbra boundary) for the 1700 Å–304 Å pair of lines. A minor discrepancy in positioning can make a contribution to the value spread for this pair of lines. The mean displacement of the circle boundaries for the 304 Å–171 Å pair of lines is about 1700 km. The propagation trajectory inclination angle  $\alpha$  was approximately estimated using a formula  $\alpha = \arctan(\Delta L / \Delta z)$ , where  $\Delta z$  is the formation level difference. To calculate phase velocities, the propagation trajectory length  $S$  is roughly derived from a formula  $S = \Delta L / \sin \alpha$ . According to our preliminary results, which were calculated taking into account the differences in line formation heights, the average inclination of the magnetic field lines is 50-55 and 55-60 degrees for the height ranges corresponding to the 1700 Å–304 Å and 304 Å–171 Å pairs of lines, respectively (Figure 4). Our estimations for the magnetic field line inclination at the umbra boundary are in compliance with the recent results from Jess *et al.* (2012) and Reznikova and Shibasaki (2012).

Direct measurements of the signal phase difference at the two height levels are hindered owing to such an extreme inclination. Wave-train structures obtained at the line of sight for the two levels do not correspond, and an unambiguous determination of the phase lag turns out to be impossible (Figure 3b). However, if we compare the signals in the points chosen with the account for the trajectory inclination, the similarity of the wave-train structures increases significantly (Figure 3a). Nevertheless, different wave trains show different phase lags. This can be caused by the uncertainties of spatial alignment.

The inclination angle is harder to estimate from the Si I–He I pair because we are dealing with a one-dimensional cut of the spot by the spectrograph entrance slit; thus we can trace only displacements along the slit. The wave-train correspondence between the two pairs of points that we had is poor.

The distributions of Si I and He I 5 min oscillation power along the slit within the umbra are peaks with maxima located close to the umbra center and minima at the umbra borders (Figure 2a). The He I peak is visibly broader than the Si I peak. The full width at half maximum of the Si I peak is 1.6 times smaller than that of the He I peak.

The 5 min oscillations in the 1700 Å and 304 Å lines are registered within the umbra, although it is not seen from the greyscale figures because the oscillation power in the penumbra is much higher than that in the umbra. The cuts along the slit of the Fe I 6173 Å (HMI) and He II 304 Å 5 min oscillation power maps (Figure 2) show the presence of peaks in the umbra, similar to those seen in the ground-based telescope observations. The displacement between the different layer umbral peaks is close to that observed for the Si I–He I pair.

The full width at the peak half maximum of the oscillation power distribution in the He I line exceeds that of the Si I line in the other frequency bands (5–8 mHz) as well (Figure 5). The ratio is 1.6 for the 5.5 mHz and decreases to 1 with frequency increasing to 7.5 mHz. There is a 2'' shift between the Si I and He I peaks in the oscillation power distributions (Figure 5, first column). The positional angle does not cause such a displacement because the spot was observed close to the disk center. In our opinion, the displacement is caused by the magnetic field inclination.

Spatial power distributions for the lower frequency oscillations are presented in Figure 6. As one can see, the 15 min oscillations are concentrated in the outer penumbra in the higher photosphere (1700 Å), forming a circle structure. This structure expands in the transition zone (304 Å). Slender elements stretching radially become evident at this level. In the end, the 15 min oscillation power distribution in the 171 Å line partially reproduces the fan picture seen in the corona. This fact gives evidence that the low-frequency oscillations of the 10–15 min periods propagate upward from the outer penumbra and reach the corona level. It is of interest that previously Verwichte *et al.* (2009) found transverse 11 min oscillations of the coronal loops above active regions, which they identified as a fast magnetoacoustic kink mode.

Spatial distribution of the high-frequency oscillations (5.5–7.5 mHz) differs from the distribution of the low-frequency oscillations (Figure 5). First, the main power is concentrated within the umbra at the upper photospheric and chromospheric levels. Second, although the oscillation region expands significantly at the 304 Å (transition region) and the 171 Å (lower corona) heights, no circle structure appears, but fragmentariness becomes more apparent. Third, the number of umbral fragments showing presence of the oscillations decreases with increasing frequency. This means that the high-frequency oscillations concentrate in special points of the umbra. According to the finding of Jess *et al.* (2012), these points are the chromospheric umbral dots with the increased oscillation power.

The power spectra (Figure 7) calculated in the different lines for the region that is cut by the slit in the sunspot umbra show that the main changes occur at

the heights from the temperature minimum (300-500 km) to the transition region (2000-2500 km). Five-minute oscillations dominate explicitly in the Fe I 6173 Å (250 km) and Si I 10827 Å (540 km) LOS velocity power spectra, whereas frequencies from 5.2 to 7 mHz dominate at the He I 10830 Å (2100 km) and 304 Å (2300 km) line formation heights. This indicates that the 3 min umbral oscillations evolve and sharply amplify directly in a chromosphere cavity (Zhugzhda, Locans, and Staude, 1985; Botha *et al.*, 2011). We obtained similar results earlier from H $\alpha$  and Fe I 6569 Å observations (Kobanov *et al.*, 2011).

Taking into account the horizontal shift of the oscillation between the layers, we measured time lags for the 5 min oscillations. For the 1700 Å–304 Å pair of lines, the value of the time lag shows a great spread from -20 s to 108 s, where negative values signify the photospheric signal lagging behind the chromospheric one. A significant spread can appear even in one spatial point at different time intervals. Reznikova *et al.* (2012) note the similar feature of time lag measurements between the oscillations above sunspots. The average lag between the Si I and He I signals is 47 s; it shows a great spread, too. The 304 Å–171 Å pair shows the time lags from -12 to 48 s, with the average value being 24 s. Poor correspondence between the signal wave trains in the layers does not mean that there are no waves propagating through the layers upward. This may signify the presence of both standing and traveling waves in the volume researched. The presence of standing waves in an object does not exclude the possibility of this object being a source of waves propagating in the surrounding medium. If the resonator boundary does not reflect the wave thoroughly, this makes it an oscillation source. The majority of oscillation sources contain resonators. The ratio between these two types of waves influences the results obtained. (see, e.g., Kobanov *et al.* (2011)). Also, this may signify that the magnetic field loops presenting in the lower layer either do not reach the upper level returning to the photosphere or divert from the line of sight significantly.

The time lag varies from 36 to 84 s and reaches 0 at some spatial points for the 1700 Å–304 Å pair in the 0.8 mHz band passes centered at 5.5, 6.5, 7.5 mHz (see Figure 8). We chose the points located above each other at the line of sight for our analysis. Because the high-frequency oscillations propagate along the vertical and close-to-vertical magnetic field lines in the central umbra, the visibility of the traveling waves is hardly influenced by a projection effect. The wave-train structure resemblance indicates that the points located at the oscillation propagation trajectory are used. Besides, wave-train visual analysis helps avoid the  $2\pi$  uncertainty, which occurs when one measures phase lags. In the 304 Å–171 Å pair, the lag varies from 12 to 24 s (see, e.g., Figure 9). One can see that the wave trains



in Figures 8 and 9 correspond to each other much better than those of the lower frequencies. This is because the higher frequencies ‘prefer’ to propagate along the vertical magnetic flux.

Taking the height difference of 1700 km for the 1700 Å–304 Å pair and 1000 km for the 304 Å–171 Å pair (Reznikova *et al.*, 2012) and bearing in mind the diversion from the vertical propagation, we found the average phase velocities to be 24 km s<sup>-1</sup> and 42 km s<sup>-1</sup> for the first and the second pair, respectively, for the frequency band centered at 3.3 mHz. For the frequencies from 5 to 8 mHz, the phase velocities are 28 km s<sup>-1</sup> and 55 km s<sup>-1</sup>, respectively. The uncertainties of these calculations are relatively great (from 20% to 60%) owing to the inconsistencies in the determined time lags.

It is of interest to note that for all the frequencies analyzed, the 304 Å line intensity oscillation amplitude exceeds appreciably those of the other lines, both at the higher and lower levels (see also Reznikova *et al.* (2012)).

We found that the phase difference between the intensity and velocity signals (I-V) for the Fe I 6173 Å and Si I 10827 Å lines is close to 90° on average (Figure 10), which is characteristic for acoustic waves under the adiabatic approximation. This difference is ambiguous and close to 180° for the upper chromosphere He I 10830 Å line at individual time intervals. The situation with the He I 10830 Å line is complicated by the fact that its profile is largely influenced by the UV radiation coming from the upper layers of the solar atmosphere. We assume that the observed waves are slow magnetoacoustic waves propagating upward along the magnetic field lines.

We believe that intensity-temperature phase relationship research in the corona is also important. To this end, we intend to implement the promising method described in Aschwanden and Boerner (2011) and Aschwanden *et al.* (2013) in our future work.

## 4 Conclusions

The spatial distribution of 5 min oscillation power looks like a circle-shape structure matching the umbra border at the photospheric level. The circle expands, and its boundaries move away from the inner penumbra border at the higher levels (304 Å and 171 Å). This indicates that 5 min oscillations propagate along appreciably inclined magnetic tubes in the spot. The inclination of the tubes reaches 50–60 degrees at the levels of the transition region and the lower corona.

While the 10–15 min oscillation power distribution shows a circle structure

at the lower layers as well, it clearly resembles fan structures at the coronal level (it is of interest to notice that the coronal-level 5 min distribution does not show such a resemblance, at least up to the 171 Å formation level). As is known, 8-15 min oscillations dominate in the photospheric and chromospheric outer penumbra (see Sigwarth and Mattig (1997); Kobanov (2000)). This indicates that these oscillations come to the corona from the lower layers of the solar atmosphere.

The main oscillation power in the 5–8 mHz range is concentrated within the umbra boundaries both at the temperature-minimum and chromospheric levels. The oscillation region covers the greater area at the transition region and at lower corona levels than that at the photospheric level. The higher frequency oscillations are concentrated in small regions inside the umbra, probably coinciding with the loop bases anchored in umbral dots.

We found no evidence of any connection between the 3 min oscillations and fan structures, at least for the 171 Å formation level. In this respect our results agree with those of Brynildsen *et al.* (2004). It is reasonable to suppose that the connection between the 3 min oscillations and fan structures is more evident in the higher coronal levels.

We deduced that the average phase velocities are  $26 \pm 15 \text{ km s}^{-1}$  and  $50 \pm 10 \text{ km s}^{-1}$  in the frequency range 3–8 mHz for the 1700 Å–304 Å and 304 Å–171 Å height levels, respectively.

To determine the phase lags of the waves between the height levels more correctly, it is necessary to take into account the inclination of the magnetic field lines, i.e., to analyze the points not taken at the line of sight but rather chosen considering the displacement in the horizontal plane. As a result, the direct phase-lag detection procedure becomes considerably more complicated. This especially applies to the low-frequency oscillations.

**Acknowledgements.** This study was supported in part by the RFBR research project No.: 12-02-33110 mol.a.ved and the Grant of the President of the Russian Federation No.: MK-497.2012.2, Russian Federation Ministry of Education and Science state contract No.: 14.518.11.7047 and agreement No.: 8407. We acknowledge NASA/SDO science team for providing the data. We acknowledge Y.M. Kaplunenko for his help in preparing the English version of the paper.

## References

Abramov-Maximov, V.E., Gelfreikh, G.B., Kobanov, N.I., Shibasaki, K., Chupin, S.A.:

- 2011, Multilevel Analysis of Oscillation Motions in Active Regions of the Sun. *Solar Phys.* **270**, 175–189. doi:10.1007/s11207-011-9716-7.
- Aschwanden, M.J., Boerner, P.: 2011, Solar Corona Loop Studies with the Atmospheric Imaging Assembly. I. Cross-sectional Temperature Structure. *Astrophys. J.* **732**, 81. doi:10.1088/0004-637X/732/2/81.
- Aschwanden, M.J., Fletcher, L., Schrijver, C.J., Alexander, D.: 1999, Coronal Loop Oscillations Observed with the Transition Region and Coronal Explorer. *Astrophys. J.* **520**, 880–894. doi:10.1086/307502.
- Aschwanden, M.J., Boerner, P., Schrijver, C.J., Malanushenko, A.: 2013, Automated Temperature and Emission Measure Analysis of Coronal Loops and Active Regions Observed with the Atmospheric Imaging Assembly on the Solar Dynamics Observatory (SDO/AIA). *Solar Phys.* **283**, 5–30. doi:10.1007/s11207-011-9876-5.
- Balthasar, H., Wiehr, E.: 1990, Oscillations of Evershed velocities and asymmetries. *Astron. Astrophys.* **237**, 243–246.
- Beckers, J.M., Tallant, P.E.: 1969, Chromospheric Inhomogeneities in Sunspot Umbrae. *Solar Phys.* **7**, 351.
- Bloomfield, D.S., Lagg, A., Solanki, S.K.: 2007, The Nature of Running Penumbra Waves Revealed. *Astrophys. J.* **671**, 1005–1012. doi:10.1086/523266.
- Bogdan, T.J., Judge, P.G.: 2006, Observational aspects of sunspot oscillations. *Royal Society of London Philosophical Transactions Series A* **364**, 313–331.
- Botha, G.J.J., Arber, T.D., Nakariakov, V.M., Zhugzhda, Y.D.: 2011, Chromospheric Resonances above Sunspot Umbrae. *Astrophys. J.* **728**, 84. doi:10.1088/0004-637X/728/2/84.
- Brynildsen, N., Maltby, P., Brekke, P., Redvik, T., Kjeldseth-Moe, O.: 2003, Search for a chromospheric resonator above sunspots. *Advances in Space Research* **32**, 1097–1102. doi:10.1016/S0273-1177(03)00312-0.
- Brynildsen, N., Maltby, P., Foley, C.R., Fredvik, T., Kjeldseth-Moe, O.: 2004, Oscillations in the Umbral Atmosphere. *Solar Phys.* **221**, 237–260. doi:10.1023/B:SOLA.0000035065.10112.fc.
- Centeno, R., Collados, M., Trujillo Bueno, J.: 2009, Wave Propagation and Shock Formation in Different Magnetic Structures. *Astrophys. J.* **692**, 1211–1220. doi:10.1088/0004-637X/692/2/1211.

- De Moortel, I., Ireland, J., Hood, A.W., Walsh, R.W.: 2002, The detection of 3 & 5 min period oscillations in coronal loops. *Astron. Astrophys.* **387**, L13–L16. doi:10.1051/0004-6361:20020436.
- Giovanelli, R.G.: 1972, Oscillations and Waves in a Sunspot. *Solar Phys.* **27**, 71.
- Jess, D.B., De Moortel, I., Mathioudakis, M., Christian, D.J., Reardon, K.P., Keys, P.H., Keenan, F.P.: 2012, The Source of 3 Minute Magnetoacoustic Oscillations in Coronal Fans. *Astrophys. J.* **757**, 160. doi:10.1088/0004-637X/757/2/160.
- Kobanov, N.I.: 2000, The properties of velocity oscillations in vicinities of sunspot penumbra. *Solar Phys.* **196**, 129–135.
- Kobanov, N.I., Makarchik, D.V.: 2004, Propagating waves in the sunspot umbra chromosphere. *Astron. Astrophys.* **424**, 671–675. doi:10.1051/0004-6361:20035960.
- Kobanov, N.I., Kolobov, D.Y., Makarchik, D.V.: 2006, Umbral Three-Minute Oscillations and Running Penumbra Waves. *Solar Phys.* **238**, 231–244. doi:10.1007/s11207-006-0160-z.
- Kobanov, N.I., Kolobov, D.Y., Sklyar, A.A., Chupin, S.A., Pulyaev, V.A.: 2009, Characteristics of oscillatory-wave processes in solar structures with various magnetic field topology. *Astronomy Reports* **53**, 957–967. doi:10.1134/S1063772909100072.
- Kobanov, N.I., Kolobov, D.Y., Chupin, S.A., Nakariakov, V.M.: 2011, Height distribution of the power of 3-min oscillations over sunspots. *Astron. Astrophys.* **525**, A41. doi:10.1051/0004-6361/200913533.
- Lites, B.W.: 1992, Sunspot oscillations - Observations and implications. In: Thomas, J.H., Weiss, N.O. (eds.) *NATO ASIC Proc. 375: Sunspots. Theory and Observations*, 261–302.
- Marsh, M.S., Walsh, R.W.: 2006, p-Mode Propagation through the Transition Region into the Solar Corona. I. Observations. *Astrophys. J.* **643**, 540–548. doi:10.1086/501450.
- Nakariakov, V.M., Ofman, L., Deluca, E.E., Roberts, B., Davila, J.M.: 1999, TRACE observation of damped coronal loop oscillations: Implications for coronal heating. *Science* **285**, 862–864. doi:10.1126/science.285.5429.862.
- O’Shea, E., Muglach, K., Fleck, B.: 2002, Oscillations above sunspots: Evidence for propagating waves? *Astron. Astrophys.* **387**, 642–664. doi:10.1051/0004-6361:20020375.

- Reznikova, V.E., Shibasaki, K.: 2012, Spatial Structure of Sunspot Oscillations Observed with SDO/AIA. *Astrophys. J.* **756**, 35. doi:10.1088/0004-637X/756/1/35.
- Reznikova, V.E., Shibasaki, K., Sych, R.A., Nakariakov, V.M.: 2012, Three-minute Oscillations above Sunspot Umbra Observed with the Solar Dynamics Observatory/Atmospheric Imaging Assembly and Nobeyama Radioheliograph. *Astrophys. J.* **746**, 119. doi:10.1088/0004-637X/746/2/119.
- Roupe van der Voort, L.H.M., Rutten, R.J., Sütterlin, P., Sloover, P.J., Krijger, J.M.: 2003, La Palma observations of umbral flashes. *Astron. Astrophys.* **403**, 277–285. doi:10.1051/0004-6361:20030237.
- Sigwarth, M., Mattig, W.: 1997, Velocity and intensity oscillations in sunspot penumbrae. *Astron. Astrophys.* **324**, 743–749.
- Thomas, J.H., Weiss, N.O.: 2008, *Sunspots and starspots*, Cambridge University Press, Cambridge, UK. ISBN 978-0-521-86003-1.
- Tsiropoula, G., Alissandrakis, C.E., Mein, P.: 2000, Association of chromospheric sunspot umbral oscillations and running penumbral waves. I. Morphological study. *Astron. Astrophys.* **355**, 375–380.
- Tziotziou, K., Tsiropoula, G., Mein, N., Mein, P.: 2006, Observational characteristics and association of umbral oscillations and running penumbral waves. *Astron. Astrophys.* **456**, 689–695. doi:10.1051/0004-6361:20064997.
- Verwichte, E., Aschwanden, M.J., Van Doorselaere, T., Foullon, C., Nakariakov, V.M.: 2009, Seismology of a Large Solar Coronal Loop from EUVI/STEREO Observations of its Transverse Oscillation. *Astrophys. J.* **698**, 397–404. doi:10.1088/0004-637X/698/1/397.
- Wang, T.J., Ofman, L., Davila, J.M., Mariska, J.T.: 2009, Hinode/EIS observations of propagating low-frequency slow magnetoacoustic waves in fan-like coronal loops. *Astron. Astrophys.* **503**, L25–L28. doi:10.1051/0004-6361/200912534.
- Zhugzhda, I.D., Locans, V., Staude, J.: 1985, Oscillations in the chromosphere and transition region above sunspot umbrae - A photospheric or a chromospheric resonator? *Astron. Astrophys.* **143**, 201–205.
- Zirin, H., Stein, A.: 1972, Observations of Running Penumbral Waves. *Astrophys. J. Lett.* **178**, L85.

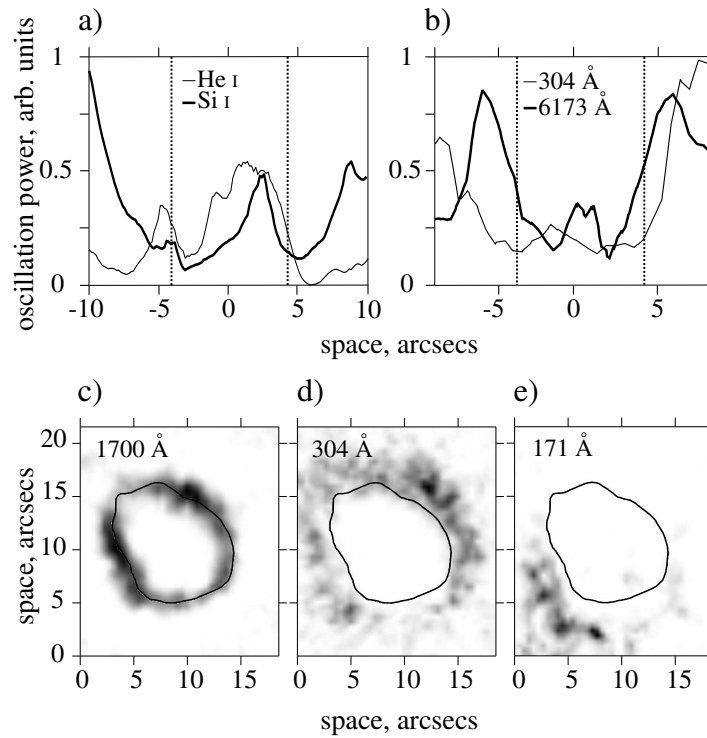


Figure 2: Spatial distribution of the 5 min oscillation power a) along the slit of the ground-based telescope (Si I 10827 Å and He I 10830 Å); b) along the slit in the 304 Å and HMI Fe I 6173 Å signals; c) in the 1700 Å continuum; d) in the 304 Å line; e) in the 171 Å line. Only the pixels with oscillation power exceeding  $3\sigma^2$  level are plotted on the distributions on the panels c–e. The darker a point, the higher is the oscillation power in it.

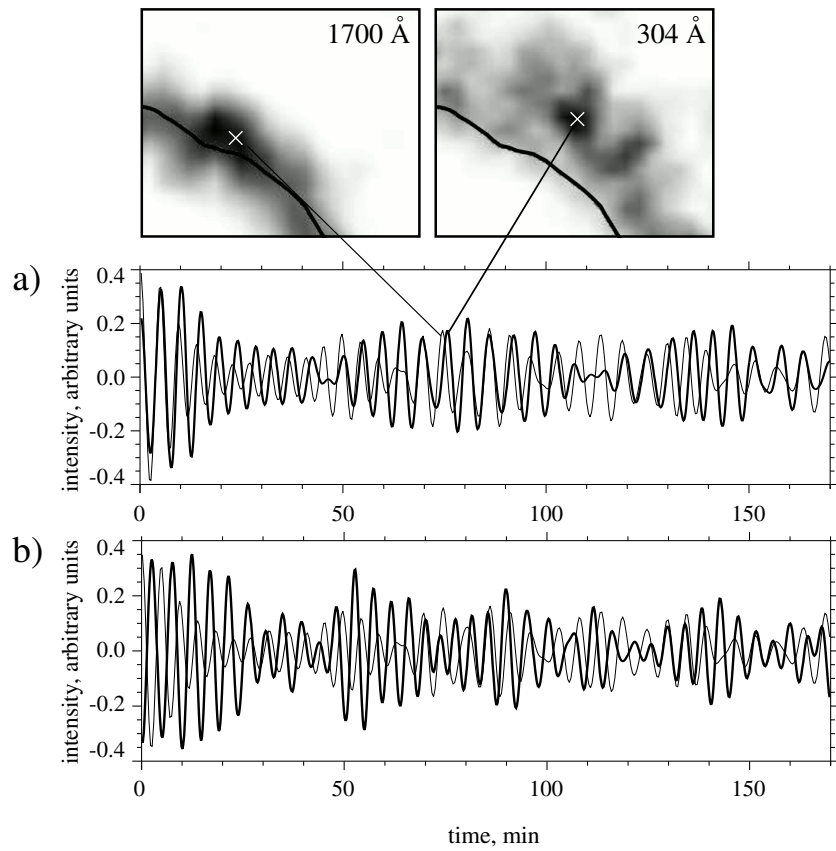


Figure 3: Phase relations between the 5 min oscillations at 1700 Å (thin) and 304 Å (thick) levels. The signals were filtered in the 0.8 mHz band centered at 3.3 mHz. a) The points for the different layers were selected accounting for the trajectory inclination, so that the filtered oscillation wave trains in the points showed the maximal correspondence (correlation coefficient is 0.7). b) The signals from the points located above each other at the line of sight at the point marked in the 1700 Å panel show less correspondence (correlation coefficient is 0.35).

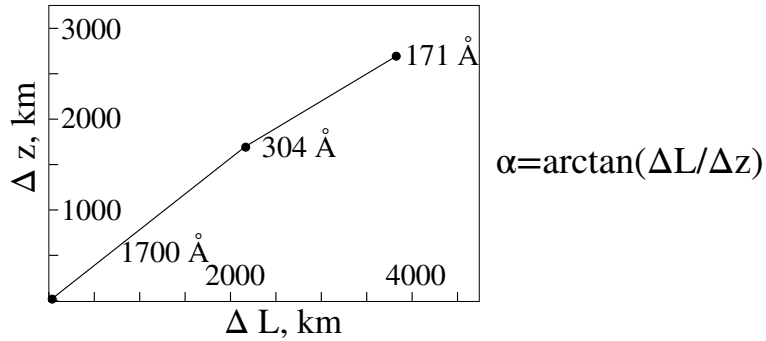


Figure 4: Graphical interpretation of the 5 min wave trajectory. The broken line represents the average magnetic field inclination to the vertical derived from the horizontal displacements ( $\Delta L$ ) and the estimations of the differences between the line formation heights ( $\Delta z$ ).

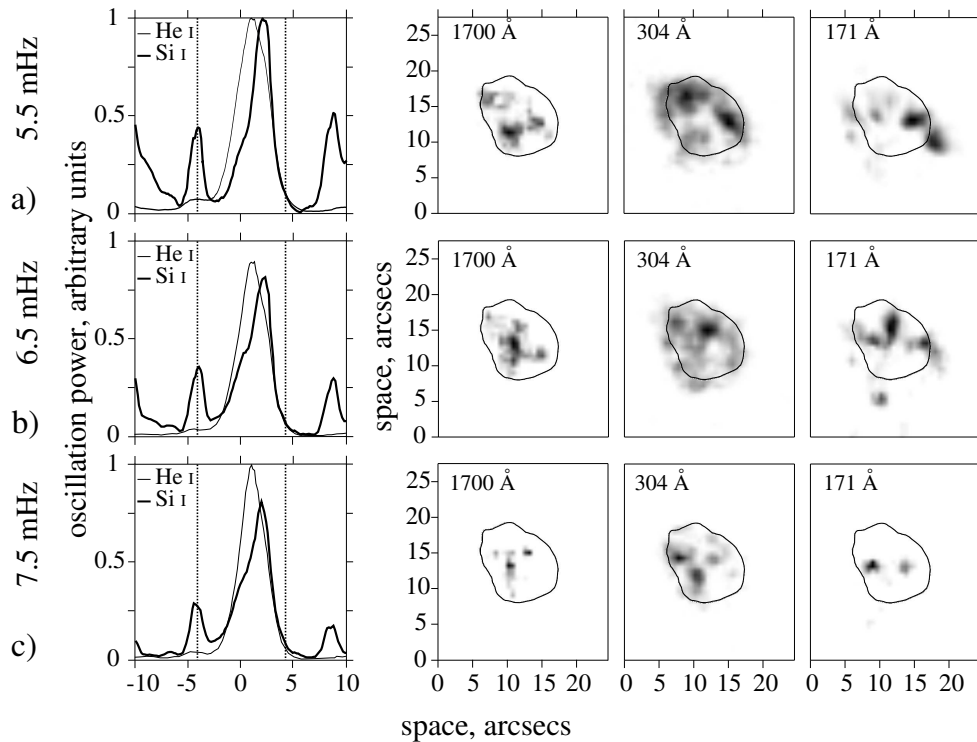


Figure 5: Oscillation power spatial distribution for the bands 0.8 mHz centered at a) 5.5 mHz; b) 6.5 mHz; c) 7.5 mHz. The first column presents the power distribution along the entrance slit for the Si I and He I lines.



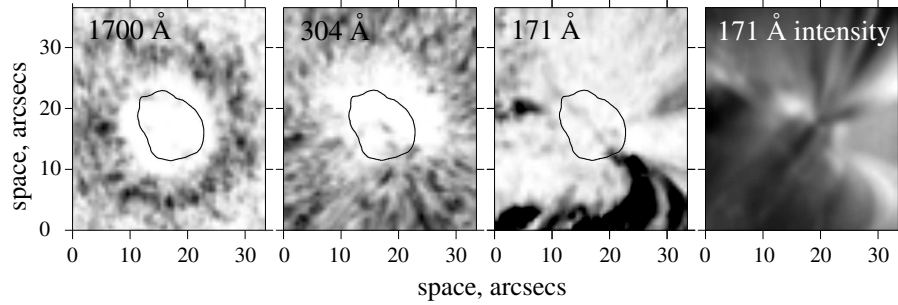


Figure 6: Propagation of the low-frequency oscillations. First three panels from left to right: spatial distribution of the 15 min oscillation power in the 1700 Å, 304 Å, and 171 Å. The fourth panel shows an image of the region in the 171 Å line intensity.

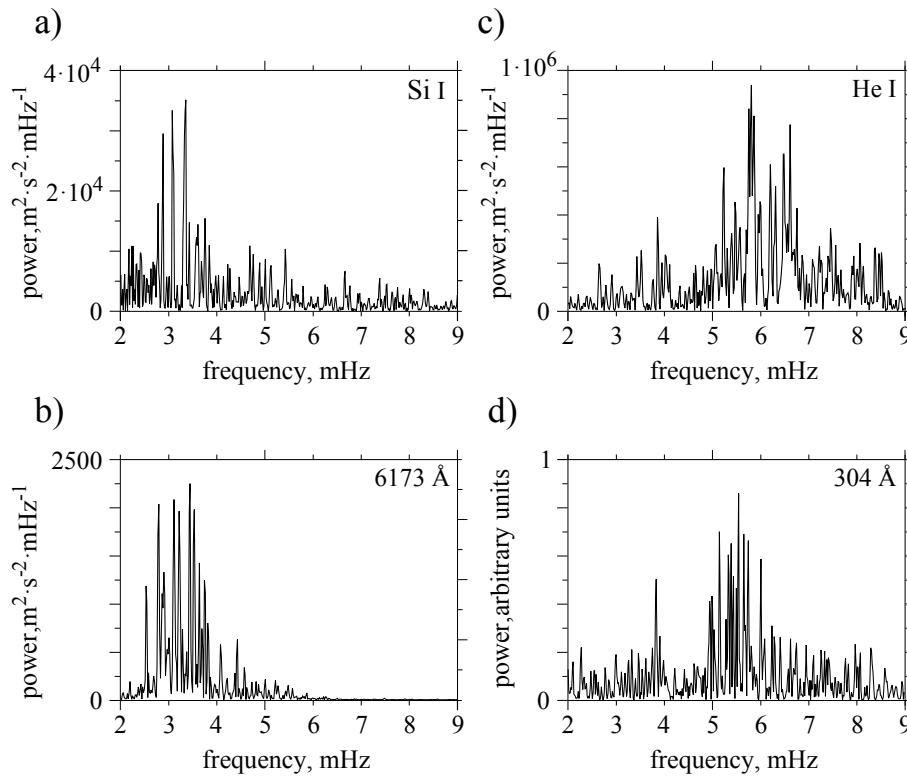


Figure 7: Umbral oscillation power spectra from the photosphere to the transition zone for the a) Si I 10827 Å LOS velocity; b) Fe I 6173 Å LOS velocity; c) He I 10830 Å LOS velocity; d) He II 304 Å intensity signal.

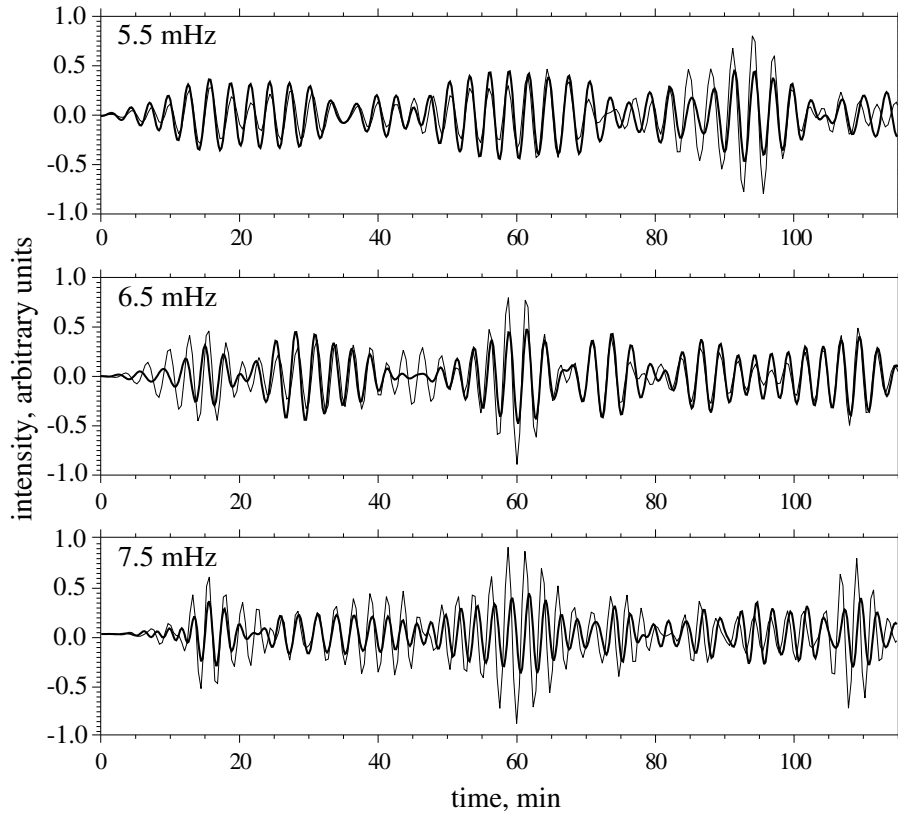


Figure 8: Signals of the 1700 Å (thin) and 304 Å (thick) lines filtered in 0.8 mHz band centered at 5.5 mHz, 6.5 mHz, and 7.5 mHz. The 304 Å signal was shifted backwards by  $\delta t$ , so that the correlation coefficients between the signals were maximal ( $\delta t$  is 36 s, 60 s, and 52 s for the upper, middle, and bottom panel, respectively). The 1700 Å signal was amplified by a factor of 3.3, 5, and 6.7 for the first, second, and third band, respectively.

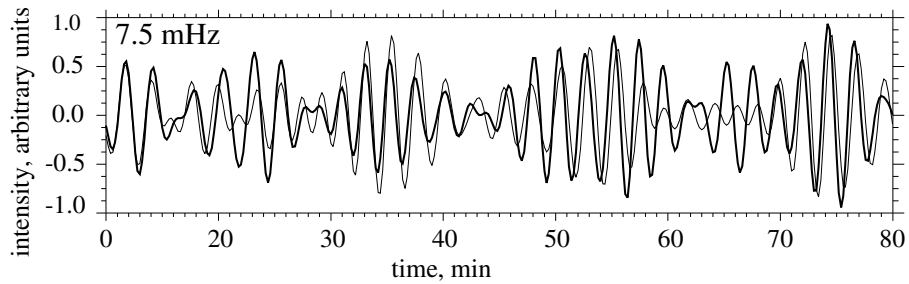


Figure 9: Unshifted signals of the 304 Å (thick) and 171 Å (thin) lines filtered in 0.8 mHz band centered at 7.5 mHz. The 171 Å signal was amplified by a factor of 2.3.

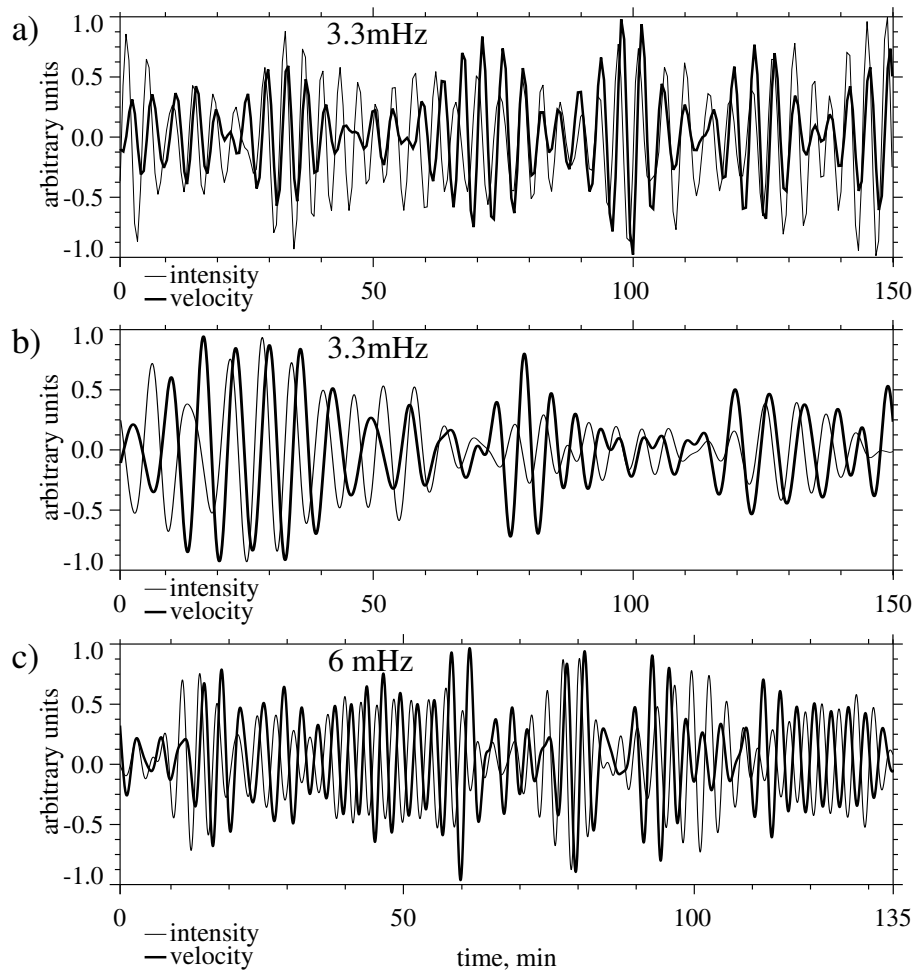


Figure 10: Phase relationships between the intensity (thin) and velocity (thick) signals for the a) Fe I 6173 Å line; b) Si I 10827 Å line; c) He I 10830 Å line.